Development of a Four-Feet Driving Type Linear Piezoelectric Actuator Using Bolt-Clamped Transducers

YINGXIANG LIU, (Senior Member, IEEE), WEISHAN CHEN, DONGDONG SHI, XINQI TIAN, SHENGJUN SHI, AND DONGMEI XU, (Student Member, IEEE)
State Key Laboratory of Robotics and System, Harbin Institute of Technology, Harbin 150001, China

Corresponding author: Yingxiang Liu (liuyingxiang868@hit.edu.cn)

ABSTRACT A four feet driving-type linear piezoelectric actuator, which achieves linear driving motion with step displacement of several microns by the alternating longitudinal motions of three bolt-clamped transducers, is designed and tested. The three transducers are located in I-shape, and the four end tips of the two horizontal transducers are used to drive the runner step-by-step. The horizontal displacements of the driving tips are used to lock the runner, whereas their vertical displacements push the runner linearly. The kinematics of the linear piezoelectric actuator is analyzed and discussed, and the deformations of the transducers are calculated. A prototype is fabricated and tested by an experimental platform. The output displacement has approximately a linear relationship with the amplitude of the voltage, and their ratio is tested to be about 0.01 μm/V. The steady displacement of the driving tip is tested to be about 1.85 μm for one step under voltage of 200 V, and a maximum speed of 141.2 μm/s is achieved under a frequency of 70 Hz.

INDEX TERMS Piezoelectric actuator, step motion, longitudinal motion, precision driving, bolt-clamped transducer.

I. INTRODUCTION

This work is within the scope of piezoelectric actuators (PAs) that have large strokes and precision driving abilities where some designs can be found in literature [1]–[6]. Two types of PAs have been developed in the past years according to their working states: the resonant type and the non-resonant type. The resonant type PAs, which are familiar to the people by the one used in the auto-focus system of Cannon camera, contain more than hundreds of different designs. For example, the classic resonant type PAs operated by the traveling waves in metal rings had been studied by many researchers [7], [8]. He *et al.* designed a novel bi-directional linear resonant type PA used the bending standing wave of a plate [9]. Kurosawa *et al.* proposed a classic V-shaped resonant type PA, their prototype achieved a maximum force of 51 N and a no-load speed of 3.5 m/s [10]. Liu *et al.* presented several successful designs on resonant type PAs with bolt-clamped structures to obtain high speeds and large forces [11], [12]. Chen *et al.* designed a two degrees-of-freedom resonant type

PA with small size [13]. The similarities of these PAs are that they achieve the actuations by the kinetic friction forces between the interfaces of the stator and the runner, and the friction forces are produced by the ultrasonic resonant vibrations of the stators. This operating principle limits the positioning accuracies of the resonant type PAs in micron scale.

Different with the resonant type PAs, the non-resonant type has higher positioning accuracy in nanometer scale as they usually achieve the positioning by the static deformations of the piezoelectric elements under DC voltages. The Physik Instrumente (PI) Company of Germany has developed a number of non-resonant type PAs used PZT stacks. The PZT stacks can achieve high positioning accuracies, but they also have shortages of small strokes as their strokes are only about 0.1% of their total lengths and usually lower than hundreds of microns. Although this stoke can be enlarged by using the amplifying mechanism, the positioning accuracy reduced proportionally [4], [14]. This problem promoted the research

of non-resonant type PAs with large strokes based on the inertia driving principle [4], [15]–[18] and the inchworm principle [1], [2], [6], [19]. These long-travel PAs with nano-positioning abilities are very useful for the fields of optical instrument, ultra-precision machining, micro-nano manufacture and cell manipulation.

The inertia driving type PAs usually push the runner step-by-step by using the slow extending and quick shortening movements of the PZT stacks. For example, Chu and Fan designed a novel long-travel nano-positioning stage used the inertia driving type PA [4]; Nomura and Aoyama proposed a micro robot with 3-DOF motions by using the inertia driving principle [15]; Peng *et al.* developed a linear micro-stage with resolution of 6 nm and total displacement of 20 mm [16]. However, the driving forces of the inertia type PAs are relatively small and backward motions of the runners are unavoidable. Cheng *et al.* proposed a very novel idea to reduce the backward motion of the inertia driving type PA by ultrasonic friction reduction [17], [18].

The inchworm PAs usually use several PZT stacks, some of them are used to lock the runner, whereas the others accomplish the driving step-by-step. Zhang and Zhu proposed a PA with positioning resolution of 5 nm and speed of 6 mm/s [20]; Ni and Zhu designed an improved PA with higher stiffness and output force [21]; Li *et al.* [22] presented a cylindrical type PA with incremental displacement of 8 μm and output force of 55 N; Kang *et al.* developed a linear PA with compact structure, positioning resolution of 10 nm, speed of 1 mm/ s and push force of 25 N [23]; Xue *et al.* designed a positioning stage with high resolution and long-travel [2]; Torii *et al.* presented an inchworm-type micro-actuator with 3-DOF driving ability [24]. The inchworm PAs usually have larger output forces than the inertia driving ones, and the backward motions of the runners are also avoidable. But one inchworm PA uses four PZT stacks at least, which means that it has high cost. Furthermore, flexure frames are commonly used in these works to protect and preload the PZT stacks, which need high precisions on the machining and assembling processes.

In this work, a four feet driving type linear piezoelectric actuator (FFDLPA), which belongs to the non-resonant type PA used the inchworm principle, is designed and tested. The scope of this FFDLPA is large stroke, high stiffness and high resolution. The bolt-clamped longitudinal transducers are used to instead of the combinations of the flexure frames and the PZT stacks in the previous designs. In detail, three longitudinal bolt-clamped transducers operated in non-resonant states are used to achieve the linear driving of a platform: two of them lock the runner alternately, while the other acts the role of the driver. The detail structure and the operating principle of the FFDLPA is discussed in Section 2, Section 3 gives the operating sequences of the transducers in alternating extensions, the experiments of a prototype are accomplished in Section 4, which is followed by a conclusion in Section 5.

II. STRUCTURE AND OPERATING PRINCIPLE

Fig. 1 gives the three-dimensional structure and the section view of the proposed FFDLPA, which can be seen as a combination of three bolt-clamped transducers. The three transducers, which are named as horizontal transducer-I, horizontal transducer-II and vertical transducer, respectively, are located in I-shape. Each transducer contains two groups of PZT ceramic plates, and the bolt-nut systems are used to clamp the PZT plates and produce compression stresses on them. The flange at the center of the vertical transducer is used for the fixing, while the four end tips of the two horizontal transducers are designed to be the driving tips. The total length, the height and the wheel base of horizontal transducer-I and II are 147 mm, 156 mm and 97 mm, respectively. Each group of PZT elements contains 30 pieces of ceramic rings with outer diameter of 25mm and thickness of 1 mm. Fig. 1(c) shows the arrangements of the ceramic rings, in which "+" and "−" are used to illustrate the polarizations. The material of the ceramic ring is PZT-5. Copper plates are placed between the ceramic rings to act as the electrodes. Each group of PZT elements is assembled separately before clamping into the transducers: epoxy adhesive is smeared uniformly on the contact surfaces of the ceramic rings and the copper plates firstly; then, they are clamped together by a precision parallel-jaw vice for about twelve hours to accomplish the solidification.

Compared with the previous linear PAs using the inchworm principle, the proposed FFDLPA has no flexure frame, and bolt bolt-clamped transducers with higher stiffness are used. Furthermore, the piezoelectric elements are not commercial PZT stacks, but self-assembled group using common PZT rings; this change not only simplifies the fabrication process, but also decreases the total cost markedly.

The operating principle of the proposed FFDLPA is illustrated by Fig. 2, in which the deformations of the piezoelectric elements and the step motions of the runners are marked by arrows. When the FFDLPA is fixed on the base by the flange, the whole cycle for the upward motions of the runners consists of the following six steps.

(1) In the first step, the two groups of ceramic elements on the horizontal transducer-I extend, which makes the two upper driving tips contact with the two runners, tightly and respectively; the other four groups of ceramic elements are all in initial states with no deformations.

(2) The two groups of ceramic elements on the vertical transducer extend under DC voltage and the two runners are pushed upward for one step by the static frictional forces generated by the two upper driving tips, while the two lower driving tips move downward freely since they are out of touch with the runners.

(3) Then, the third step enters by applying DC voltage on the ceramic elements of the horizontal transducer-II, under which the runners are held by four tips together.

(4) In the fourth step, the voltage applied on the ceramic elements on the horizontal transducer-I is removed and this
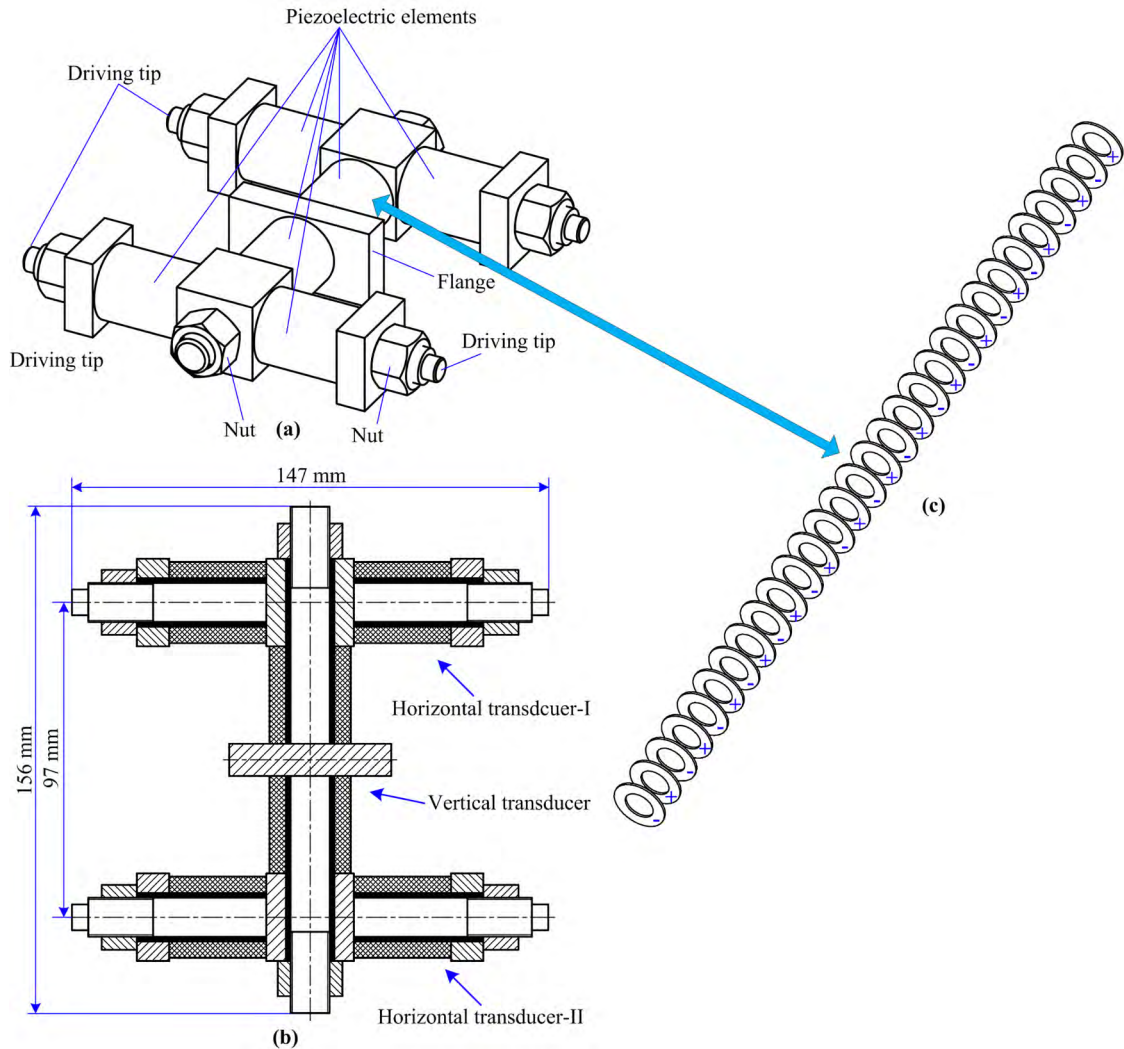
FIGURE 1. Structure of the proposed FFDLPA: (a) the three-dimensional structure, (b) the sectional view, and (c) the arrangements of the PZT ceramics for one group of piezoelectric elements.

transducer is released to its initial length; in other words, the two upper driving tips depart from the two runners, respectively.

(5) The voltage applied on the ceramic elements on the vertical transducer-I is removed in the fifth step. The vertical transducer shortens to the initial state, and the runners are pushed upward for another step.

(6) The sixth step, in which the ceramic elements on the two horizontal transducers extend together, is a transition. The difference between this step and step-3 is that the vertical transducer is in free state.

The repetitions of (1)–(2)–(3)–(4)–(5)–(6) can move the runner with long-travel; the stroke is mainly decided by the length of the runner. In the whole cycle, the runners are held tightly and stably by two or four driving tips, which are very significant for the accurate positioning. Furthermore, the runners are pushed by the static frictional forces, which means that there will be no wear and tear problems.

Similarly, the downward actuating of this FFDLPA will be realized by generating the ceramic elements in sequences of (1)–(6)–(5)–(4)–(3)–(2); the different point is that the step motions of the runner will be accomplished under step-4 and step-1, respectively.

III. DEFORMATIONS OF THE TRANSDUCERS AND MOVEMENT OF THE DRIVING TIP

Finite element method (FEM) was used in this study to calculate the deformations of the transducers in the proposed FFDLPA. The FEM model of the FFDLPA, as shown in Fig. 3, was developed in ANSYS software. Fixed boundary conditions were applied on the two side surfaces of the flange. DC voltages were applied on the ceramic rings to obtain the deformations of the transducers and the static displacements of the driving tips. The deformations corresponded to the six steps shown in Fig.2 were calculated one by one, as shown in Fig. 4.
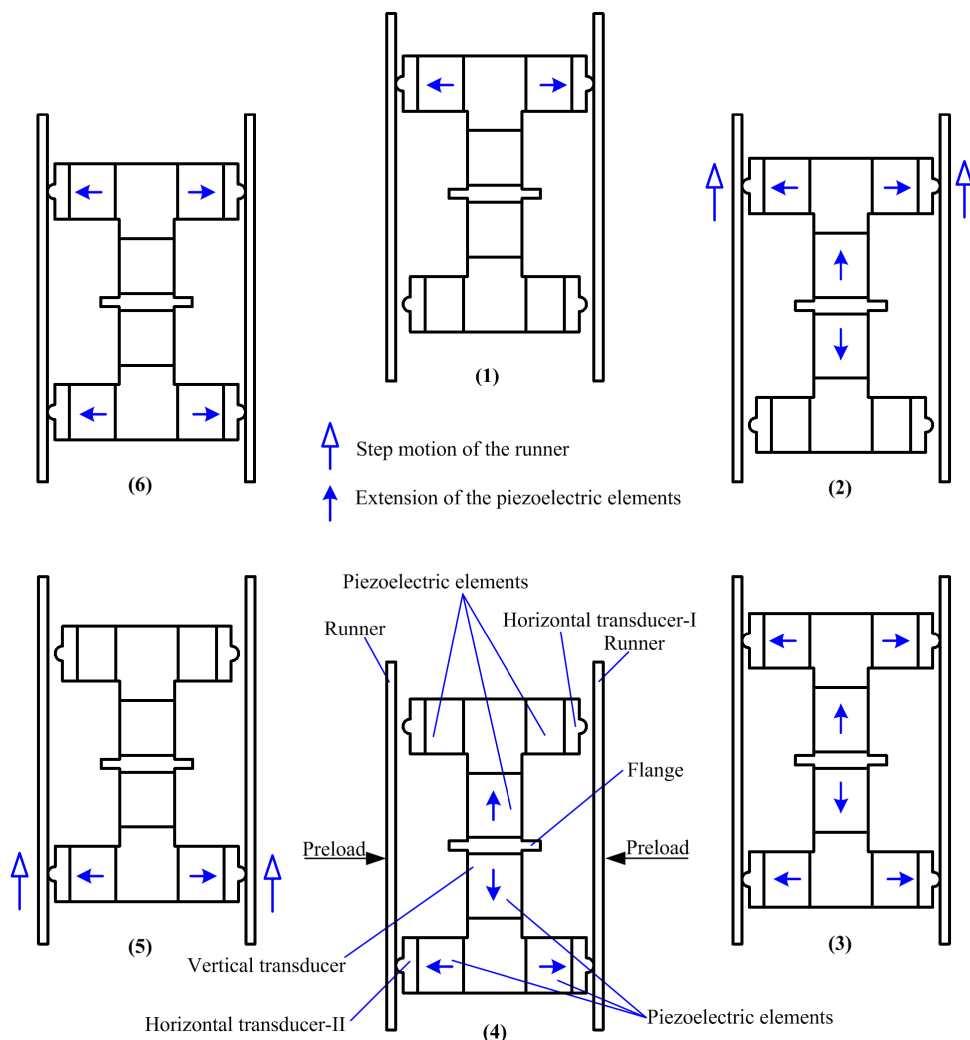
FIGURE 2. Operating principle of the proposed FFDLPA in one period.

In Fig. 4, the initial un-deformed edge of the FEM model is also plotted to give a clear comparison. The vibration shape shown in Fig. 4(1) is gained by applying DC voltage of 200 V on the ceramic elements of the horizontal transducer-I; this vibration shape is in good agreement with the one shown in Fig. 2(1). The other five vibration shapes are calculated according to the steps discussed above, during which DC voltages are applied in order to produce the desired deformations, both vertically and horizontally.

The static analysis shows that the vertical displacements of the driving tips are about 2.08 μm under voltage of 200 V, whereas the horizontal displacements are about 1.95 μm. The difference between these two values is mainly caused by the discrepancy of the lengths of the bolts used in the transducers. The bolt used in the vertical transducer is longer than that of the one in the horizontal transducer, which allows the vertical transducer to extend longer under the same axial force produced by the PZT elements. Fig. 5 gives the movement trajectory of one driving tip, which is a rectangle motion, and
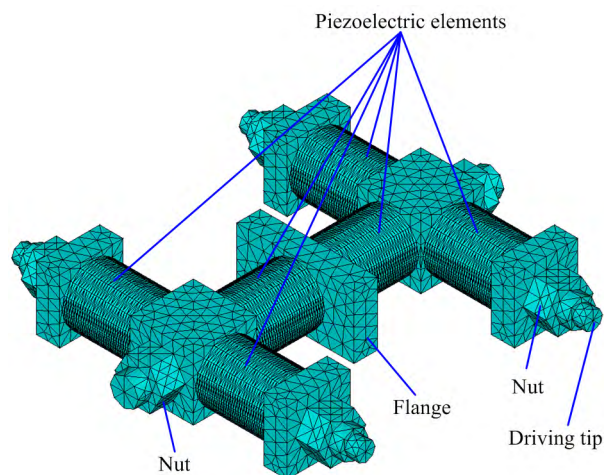

FIGURE 3. FEM model of the proposed FFDLPA.

the driving tip will stop at the four corners sequentially under different movement steps.
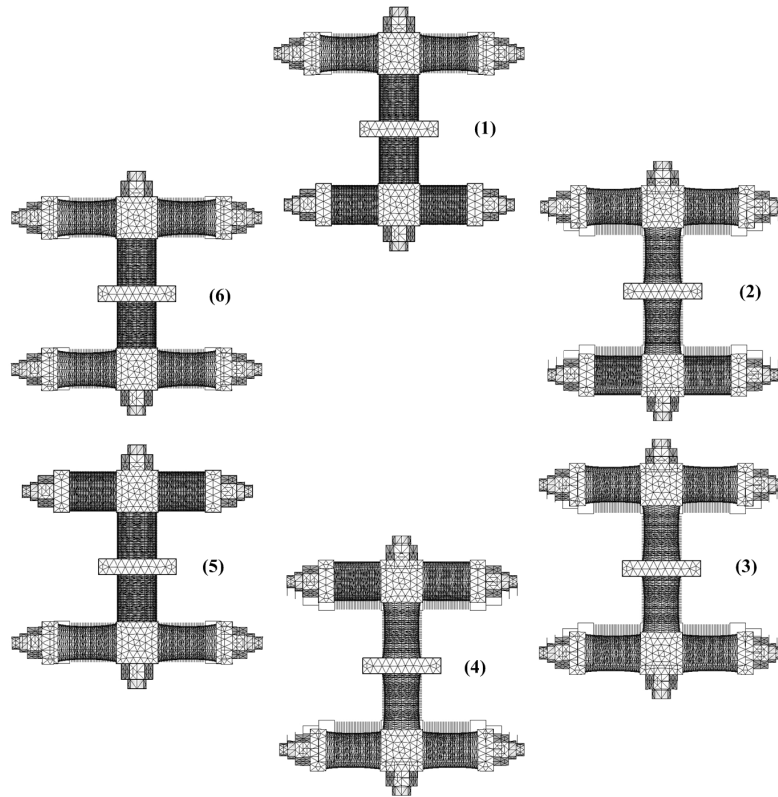
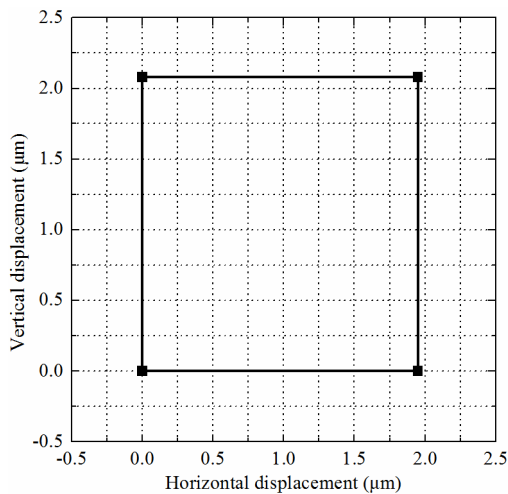**FIGURE 4.** Vibration shape changes of the proposed FFDLPA in one period.

FIGURE 5. Movement trajectory of one driving tip.

FIGURE 6. Transient responses of the vertical displacement of the driving tip.

Then, the transient responses of the horizontal and vertical displacements of the driving tip were calculated by the ANSYS software. The transient responses of the displacements under the step signal with amplitude of 200V were obtained, as shown in Fig. 6. It is found that the driving tip takes about 2 ms to reach the maximum displacement, and then come to the steady state quickly after minute oscillations. The steady vertical and horizontal displacements reach about
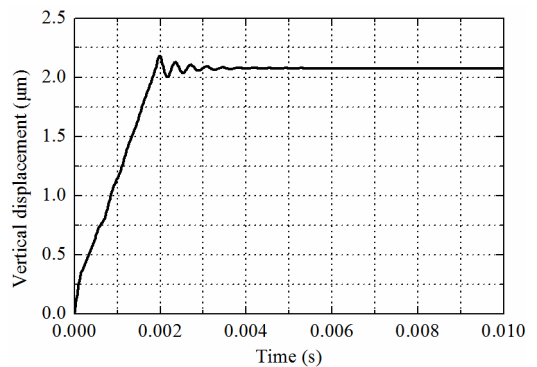
2.08 μm and 1.95 μm, respectively, which agree well with the static analysis results.

IV. EXPERIMENTS
A prototype of the proposed FFDLPA was fabricated, and a linear platform was designed and fabricated to test the mechanical output performance of the FFDLPA. A capacitive displacement senor (D-E20.200, PI, Germany) was used to measure the displacement of the runner. The thrust force of the prototype was measured by linking a weight with the runner though a wheel-string system, and the gravity of the
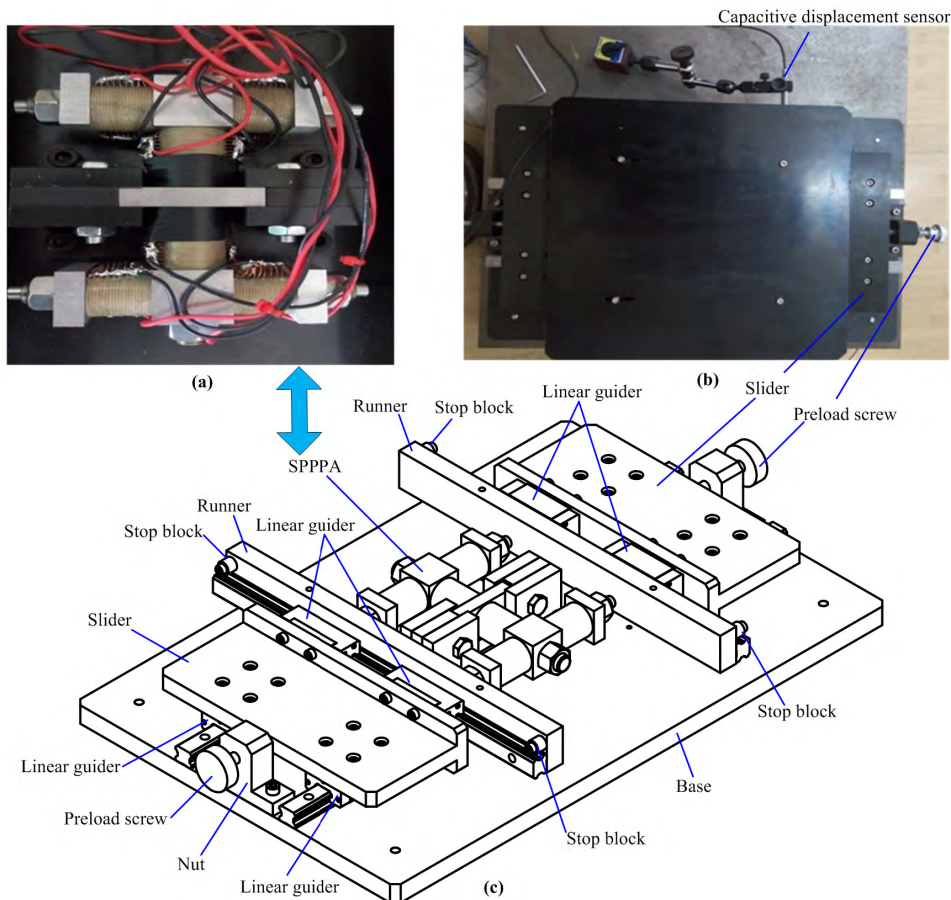
FIGURE 7. Prototype of the proposed FFDLPA and the experiment set-up: (a) the photo of the FFDLPA, (b) the photo of the platform, and (c) the three-dimensional structure of the linear platform used the FFDLPA.

weight was seen as the output thrust force. The prototype of the FFDLPA and the linear platform are shown in Fig. 7.

Firstly, we measured the displacement responses of the driving tip in time domain under no-load condition by removing the runner system. The vertical and horizontal displacements were measured separately by placing the senor to face the end surfaces of the vertical and horizontal transducers, respectively. The transient responses of the displacements under different DC voltages were measured and plotted, see Fig. 8.

It is found that the transducers take about 2 ms to reach the maximum displacement, and then turn to relative steady states after short oscillation processes. The tested response time agrees well with the calculated one shown in Fig. 6, which proves that the simulation results by the FEM have enough accuracy. It should be noted that the final states of horizontal and vertical displacements are not stable totally, and their noises are mainly caused by the uncontrolled vibrations from the environment since no vibration isolation platform is used during the measurement. The noise in the horizontal displacement is higher than that of the vertical displacement. The difference between the noises of the horizontal and vertical displacements is mainly caused by the difference of their

boundary conditions. This actuator is fixed on the base by the flange of the vertical transducer, which means that the vertical transducer has a firmer boundary than the horizontal transducer. The average vertical displacements in the steady states are about 0.47 μm, 0.96 μm, 1.54 μm and 2.08 μm under DC voltages of 50 V, 100 V, 150 V and 200 V, while the corresponding values for the horizontal displacement are 0.48 μm, 0.95 μm, 1.47 μm and 2.01 μm, respectively. The tested displacements are very close to the calculated values by FEM. Fig. 9 plots the vertical and horizontal displacements in ten cycles (the voltage is 200V), which states that the transducers have good repetitiveness on the extended motions. The mean values of the horizontal and vertical displacements of the ten cycles are about 2.075 μm and 2.006 μm, while the errors between the horizontal and vertical mean values are about 0.020 μm and 0.019 μm, respectively.

Then, the runner system was assembled and the output performances of the prototype were measured. The output displacements of the platform were measured under different DC voltages applied on the vertical transducer, as shown in Fig. 10. The amplitude of voltage shows nearly a linear effect on the output displacement and their ratio is about 0.01 μm/V. It means that a output resolution of 1nm can
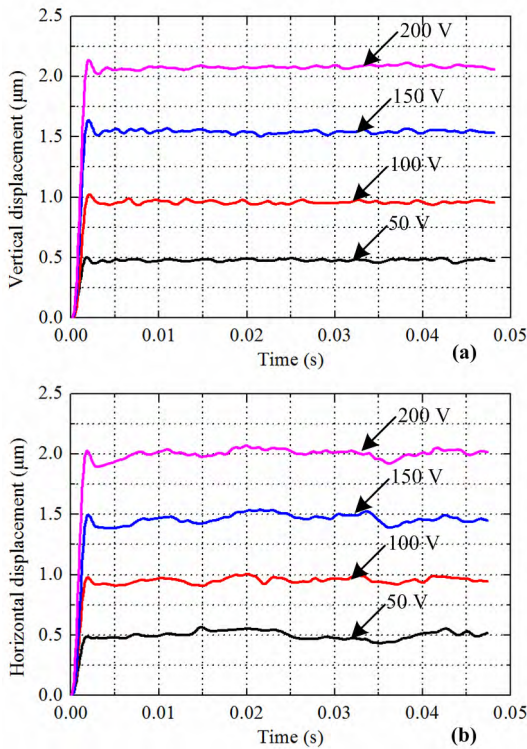
FIGURE 8. Transient responses of the displacements of the driving tip: (a) vertical direction and (b) horizontal direction.

FIGURE 9. Repetitiveness of the displacements of the driving tip: (a) vertical direction and (b) horizontal direction.

FIGURE 10. Plot of the output displacement versus the amplitude of the applied DC voltage.

be achieved under input voltage with resolution of 0.1 V. The resolution of the capacitive displacement senor is 2 nm, but a minimum output displacement of 20 nm is obtained under the input voltage of 2V. However, this minimum output displacement can reach smaller theoretically by improving the test environment. The output displacement verifies that the FFDLPA has the output ability with nanometer resolution, and it can be potentially operated in nanometer level accuracy under a proper close-loop control.

Fig. 11(a) shows the step-by-step motion of the runner in time domain, which is tested under voltage of 200V and frequency of 20 Hz. Within time of 0.4 s, the prototype accomplishes eight circles and the runner is pushed linearly for 16 steps; the runner moves about 29.6 μm, which means that the mean value of each step is about 1.85 μm, and the maximum error between the 16 steps is about 0.01 μm. The tested step distance is a little lower than the vertical displacement of the driving tip under no-load condition. It is observed that there are two small peaks located in the steady-state of each steps: in the odd steps the peaks are upward, while downward peaks occur in the even steps. These small peaks are mainly caused by the changes of the contact states between the driving tips and the runners. The vibration shape changes shown in Fig. 4 can be used to explain this problem. Specifically speaking, the steady-states of the runners are realized by keeping the length of vertical transducer under a fixed value, but the contact states between the driving tips and the runners change during this process: step (2) shows that
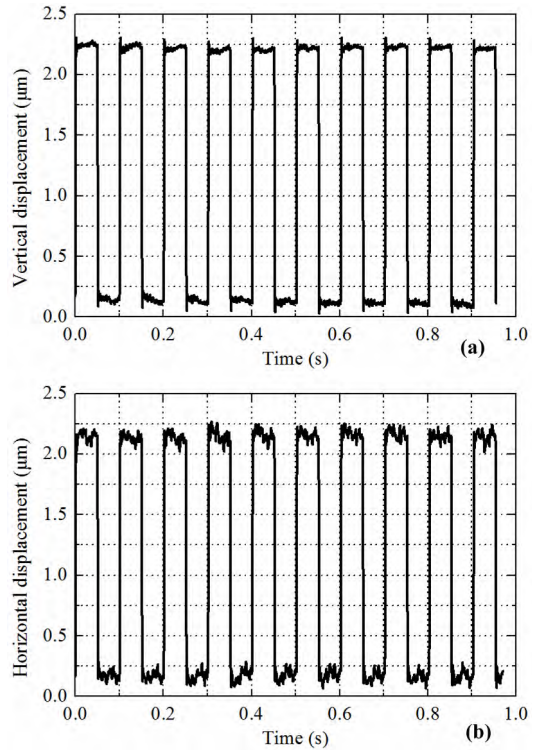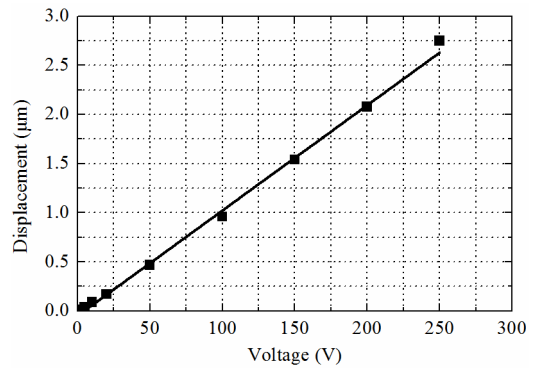
the runners are locked by the horizontal transducer-I, step (3) shows that the runners are locked by the two horizontal transducers, step (4) shows that the runners are locked by the horizontal transducer-II. Thus, the contact states between the driving tips and the runners change two times in one step, which causes the appearances of the small peaks.

Fig. 11(b) shows the effect of the voltage on the output speed under frequency of 20 Hz: the runner gets very low speeds under voltages lower than 40 V and moves stably under voltages above 50 V, a maximum speed of 88 μm/s is achieved under voltage of 250 V. The horizontal and vertical transducers used voltages with the same amplitude during the measurement for the simplification of the power supply. This phenomenon states that the horizontal transducers need
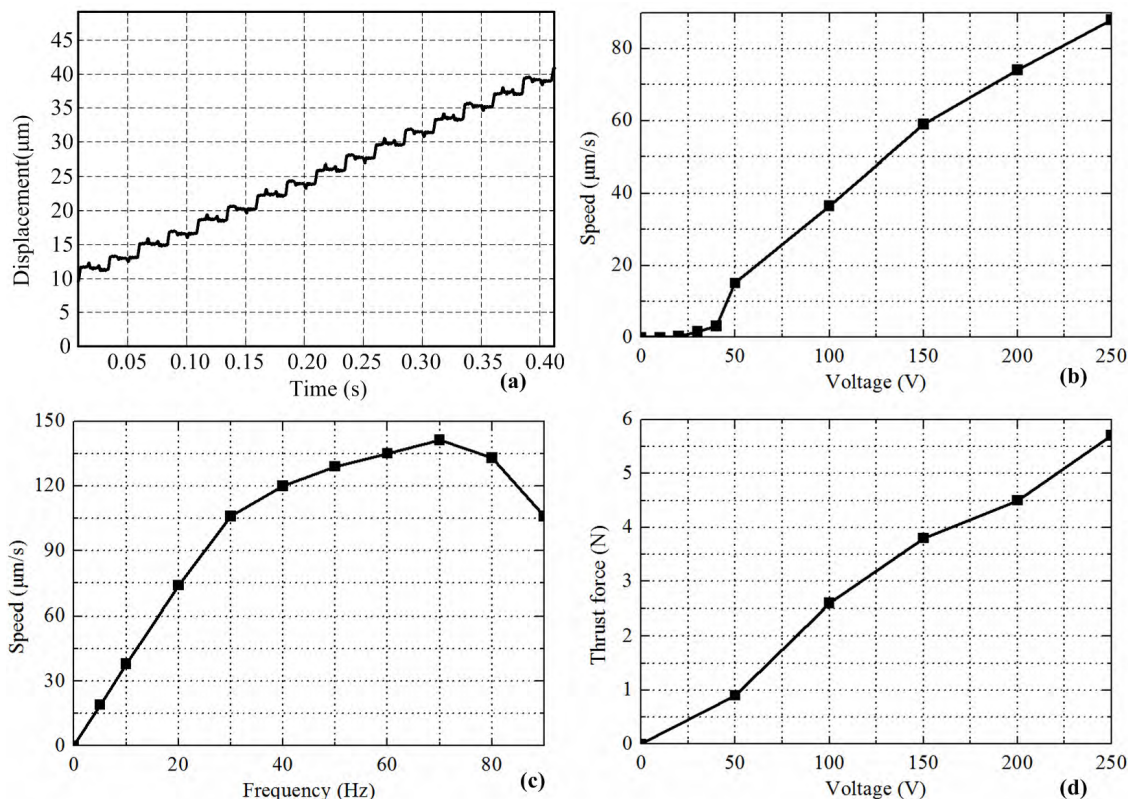
FIGURE 11. Mechanical output performance of the prototype: (a) plot of the step-by-step displacement in time domain, (b) plot of the no-load speed versus the amplitude of the voltage, (c) plot of the no-load speed versus the frequency of the voltage, and (d) plot of the output force versus the amplitude of the voltage.

voltage of 50 V at least to produce enough locking force for the runner. Theoretically speaking, the voltage applied on the vertical transducer can be tuned to a value lower than 50V to drive the runner with a lower speed.

The relationship between the frequency and the output speed is plotted in Fig. 11(c): linear effect appears in frequency region from 5 Hz to 30 Hz, the increase of the speed turns to slow down from 30 Hz to 70 Hz, and the decrease of the speed occurs when the frequency is higher than 70 Hz. A maximum speed of 141.2 μm/s is achieved under frequency of 70 Hz and voltage of 200 V. At last, the out thrust force was measured under different voltages, as shown in Fig. 11(d); a maximum force of 5.7 N was reached under voltage of 250 V.

Although this FFDLPA achieves lower speed and smaller thrust by comparing with the inchworm type actuator designed by Xue *et al.* in reference 2, it improves the displacement resolution obviously: the resolution of the FFDLPA is 20 nm, while the resolution of Xue's actuator is 40 nm. Furthermore, the FFDLPA in this work has features as follow by comparing with the previous linear PAs using the inchworm principle.

(1) The proposed FFDLPA has higher stiffness and high resonance frequency by using the bolt-clamped transducers. Generally speaking, higher resonance frequency means better

performance on dynamic characteristics. Usually, the flexure frames used in the previous designs contain thin beams with low stiffness. It is well known that the thin beam structure always has very low resonance frequency. The first resonance frequency of the FFDLPA is calculated to be about 710 Hz by FEM modal analysis. It should be noted that this resonance frequency is not conflicted with the tested working frequency of 70 Hz for the maximum output speed shown in Fig. 11(c). The actual working frequency of the prototype should be lower than the first resonance frequency of the FFDLPA as it works under the non-resonant state. Usually, the maximum working frequency should lower than one-third of the first resonance frequency, which means that the prototype can be operated under a maximum frequency of about 237 Hz. Theoretically speaking, the prototype can achieve higher maximum speed under higher working frequency by reducing the weight of the runner, which means that the weight of the runner in the experiment limits the maximum working frequency at 70 Hz. The proposed FFDLPA has a first resonance frequency of 710 Hz, which means that it will have better stability under the environmental low frequency vibrations by comparing with the previous designs with lower resonance frequencies. Furthermore, there is very weak problem of heating as the proposed FFDLPA works under the non-resonant state, which makes it has a long life and high

durability. The FFDLPA exhibits very good durability during the experiments, and it has the same output performance after working for dozens of hours.

(2) The piezoelectric elements are self-assembled groups using common PZT plates, they cost only about 17% of the commercial PZT stacks, which makes the FFDLPA very suitable for the design of linear precision PA with low cost. For the fabrication of each group of PZT elements, 30 pieces of ceramic rings are bonded together, and it costs about 600 Chinese Yuan (CNY) since the price of one ceramic ring is only about 20 CNY. In comparison, the commercial PZT stack with the same dimensions may cost over 3500 CNY.

V. CONCLUSION

A four feet driving type FFDLPA with long travel output ability was proposed and tested. The axial extensions of three bolt-clamped transducers were used to produce rectangle movements on the driving tips: the horizontal displacement was used to lock the runner, whereas the vertical one drove the runner linearly step-by-step. The bolt-clamped structure used in this design gained high stiffness as the first resonance frequency was calculated to be about 710 Hz. The experiments accomplished by the prototype verified the proposed idea, and a step displacement of 1.85 μm was reached under voltage of 200 V. The speed of the runner increased with the frequency, and reached the maximum value of 141.2 μm/s at 70 Hz. The proposed FFDLPA can achieve precision positioning in nanometer scale as the vertical displacement of the driving tip can be tuned in high resolution by using a power with accurate voltage adjustment ability, which will be the research focus of the following work. It should be noted that the mechanical output performances are measured under open-loop control condition, and the following works will also focus on the development of a proper close-loop control method to improve the position accuracy. The proposed FFDLPA has large potentials for applications in fields such as optical instrument, precision machining, nanometer manipulation, etc; we will also focus on its applications in these fields in the following works.

REFERENCES

[1] P. E. Tenzer and R. B. Mrad, "A systematic procedure for the design of piezoelectric inchworm precision positioners," *IEEE/ASME Trans. Mechatronics*, vol. 9, no. 2, pp. 427–435, Jun. 2004.

[2] X. Xue, X. Tian, D. Zhang, and X. Liu, "Design of a piezo-driven inchworm flexure stage for precision positioning," *Int. J. Appl. Electromagn. Mech.*, vol. 50, no. 4, pp. 569–581, 2016.

[3] J. Kim and J.-H. Lee, "Self-moving cell linear motor using piezoelectric stack actuators," *Smart Mater. Struct.*, vol. 14, no. 5, pp. 934–940, 2005.

[4] C.-L. Chu and S.-H. Fan, "A novel long-travel piezoelectric-driven linear nanopositioning stage," *Precis. Eng.*, vol. 30, no. 1, pp. 85–95, 2006.

[5] D. Xu, Y. Liu, J. Liu, S. Shi, and W. Chen, "Motion planning of a stepping-wriggle type piezoelectric actuator operating in bending modes," *IEEE Access*, vol. 4, pp. 2371–2378, 2016.

[6] S. P. Salisbury, D. F. Waechter, R. B. Mrad, S. E. Prasad, R. G. Blacow, and B. Yan, "Design considerations for complementary inchworm actuators," *IEEE/ASME Trans. Mechatronics*, vol. 11, no. 3, pp. 265–272, Jun. 2006.

[7] S. Li, W. Ou, M. Yang, C. Guo, C. Lu, and J. Hu, "Temperature evaluation of traveling-wave ultrasonic motor considering interaction between temperature rise and motor parameters," *Ultrasonics*, vol. 57, pp. 159–166, Mar. 2015.

[8] Y. Ting, L.-C. Chen, C.-C. Li, and J.-L. Huang, "Traveling-wave piezoelectric linear motor. I. The stator design," *IEEE Trans. Ultrason., Ferroelect., Freq. Control*, vol. 54, no. 4, pp. 847–853, Apr. 2007.

[9] S. He, W. Chen, X. Tao, and Z. Chen, "Standing wave bi-directional linearly moving ultrasonic motor," *IEEE Trans. Ultrason., Ferroelect., Freq. Control*, vol. 45, no. 5, pp. 1133–1139, Sep. 1998.

[10] M. K. Kurosawa, O. Kodaira, Y. Tsuchitoi, and T. Higuchi, "Transducer for high speed and large thrust ultrasonic linear motor using two sandwich-type vibrators," *IEEE Trans. Ultrason., Ferroelect., Freq. Control*, vol. 45, no. 5, pp. 1188–1195, Sep. 1998.

[11] Y. Liu, W. Chen, X. Yang, and J. Liu, "A rotary piezoelectric actuator using the third and fourth bending vibration modes," *IEEE Trans. Ind. Electron.*, vol. 61, no. 8, pp. 4366–4373, Aug. 2014.

[12] Y. Liu, W. Chen, J. Liu, and X. Yang, "A high-power linear ultrasonic motor using bending vibration transducer," *IEEE Trans. Ind. Electron.*, vol. 60, no. 11, pp. 5160–5166, Nov. 2013.

[13] Z. Chen, X. Li, G. Liu, and S. Dong, "A two degrees-of-freedom piezoelectric single-crystal micromotor," *J. Appl. Phys.*, vol. 116, no. 22, 2014, Art. no. 224101.

[14] P. A. Sente, F. M. Labrique, and P. J. Alexandre, "Efficient control of a piezoelectric linear actuator embedded into a servo-valve for aeronautic applications," *IEEE Trans. Ind. Electron.*, vol. 59, no. 4, pp. 1971–1979, Apr. 2012.

[15] Y. Nomura and H. Aoyama, "Development of inertia driven micro robot with nano tilting stage for SEM operation," *Microsyst. Technol.*, vol. 13, pp. 1347–1352, May 2007.

[16] Y.-X. Peng *et al.*, "A linear micro-stage with a long stroke for precision positioning of micro-objects," *Nanotechnol. Precis. Eng.*, vol. 9, pp. 221–227, May 2011.

[17] T. Cheng, H. Li, M. He, H. Zhao, X. Lu, and H. Gao, "Investigation on driving characteristics of a piezoelectric stick–slip actuator based on resonant/off-resonant hybrid excitation," *Smart Mater. Struct.*, vol. 26, no. 3, p. 035042, 2017.

[18] T. Cheng *et al.*, "Performance improvement of smooth impact drive mechanism at low voltage utilizing ultrasonic friction reduction," *Rev. Sci. Instrum.*, vol. 87, no. 8, p. 085007, 2016.

[19] J. Kim, H.-K. Kim, and S.-B. Choi, "A hybrid inchworm linear motor," *Mechatronics*, vol. 12, no. 4, pp. 525–542, 2002.

[20] B. Zhang and Z. Zhu, "Developing a linear piezomotor with nanometer resolution and high stiffness," *IEEE/ASME Trans. Mechatronics*, vol. 2, no. 1, pp. 22–29, Mar. 1997.

[21] J. Ni and Z. Zhu, "Design of a linear piezomotor with ultra-high stiffness and nanoprecision," *IEEE/ASME Trans. Mechatronics*, vol. 5, no. 4, pp. 441–443, Dec. 2000.

[22] J. Li, R. Sedaghati, J. Dargahi, and D. Waechter, "Design and development of a new piezoelectric linear Inchworm actuator," *Mechatronics*, vol. 15, no. 6, pp. 651–681, 2005.

[23] D. Kang, M. G. Lee, and D. Gweon, "Development of compact high precision linear piezoelectric stepping positioner with nanometer accuracy and large travel range," *Rev. Sci. Instrum.*, vol. 78, no. 7, p. 075112, 2007.

[24] A. Torii, M. Nishio, K. Doki, and A. Ueda, "A 3-DOF inchworm using levitation caused by vertical vibration," *Elect. Eng. Jpn.*, vol. 196, no. 1, pp. 22–30, 2016.
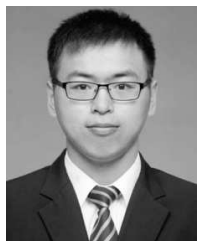
YINGXIANG LIU (M'12–SM'16) was born in Hebei Province, China, in 1982. He received the B.E., M.E., and Ph.D. degrees from the School of Mechatronics Engineering, Harbin Institute of Technology, China, in 2005, 2007, and 2011, respectively. He joined the School of Mechatronics Engineering, Harbin Institute of Technology in 2011, where he has been a Professor since 2013. He was a Visiting Scholar with the Mechanical Engineering Department, University of California, Berkeley, from 2013 to 2014. He is currently a Professor with the School of Mechatronics Engineering, Harbin Institute of Technology. He is also the Vice Director of the Department of Mechatronic Control and Automation. He is also a member of the State Key Laboratory of Robotics and System, Harbin Institute of Technology. His research interests include piezoelectric actuating, ultrasonic motor, piezoelectric actuator, precision actuating, piezoelectric micro jet, bionic robot, fish robot, and soft robot. He has served as an Associate Editor of the IEEE Access.

WEISHAN CHEN was born in Hebei Province, China in 1965. He received the B.S. and M.S. degrees in precision instrumentation engineering and the Ph.D. degree in mechatronics engineering from the Harbin Institute of Technology, China, in 1986, 1989, and 1997, respectively. Since 1999, he has been a Professor with the School of Mechatronics Engineering, Harbin Institute of Technology. His research interests include ultrasonic driving, smart materials and structures, and bio-robotics.
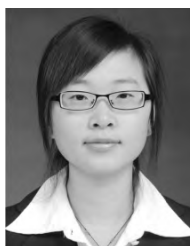
DONGDONG SHI was born in Hebei Province, China in 1991. He received the B.S. and M.S. degrees from the School of Mechatronics Engineering, Harbin Institute of Technology, China, in 2014 and 2016, respectively. His research interests include ultrasonic motor and ultra-precision piezoelectric actuating.

XINQI TIAN was born in Inner Mongolia Province, China in 1992. He received the B.E. and M.E. degrees from the School of Mechatronics Engineering, Harbin Institute of Technology, China, in 2014 and 2016, respectively, where he is currently pursuing the Ph.D. degree. His research interests include ultrasonic motor and precision piezoelectric actuating.

SHENGJUN SHI was born in Heilongjiang Province, China in 1974. He received the B.S. degree in aircraft manufacturing engineering form Northwest Polytechnical University in 1997 and the M.S. and Ph.D. degrees from the School of Mechatronics Engineering, Harbin Institute of Technology, China, in 2003 and 2007, respectively. He is currently an Associate Professor with the Harbin Institute of Technology. His research interests include ultrasonic motor and ultrasonic application.

DONGMEI XU (S'15) was born in Shandong Province, China in 1987. She received the B.S. degree from the College of Mechanical and Electrical Engineering, Yantai University, China, in 2010, and the M.S. degree from the School of Mechatronics Engineering, Harbin Institute of Technology, China, in 2012, where she is currently pursuing the Ph.D. degree. Her research interests include ultrasonic motor and ultra-precision piezoelectric actuating.

• • •